Study on the thermal decomposition reaction process and kinetics of SF6 and tungsten

Mengyuan Xu[1], Houhua Lv[2], Yunfang Liu[5], Ren Yang[1], Yanhua Han[1], Liuyu Xu[3], Xu Li[4], Jiuhong Li[1], Xiao Zhang[2] , Yajun Jian[2*], Weiqiang Zhang[2, *]

[1]State Grid Shaanxi Electric Power Research Institute, 710054, Xi'an, China
[2]School of Chemistry and Chemical Engineering, Shaanxi Normal University, 710119, Xi'an, China
[3]Shandong Taikai High Voltage Switchgear Co.,Ltd., 271000, Tai'an, China
[4]State Grid Shaanxi Electric Power Company, 710054, Xi'an, China
[5]South China Institute of Environmental Science, Ministry of Ecology and Environment, 510655, Guangzhou, China

Abstract The thermal reaction of SF_6 with tungsten powder was investigated by thermogravimetry (TG) and differential scanning calorimetry (DSC), combined with the characterization of solid decomposition products of SF_6 and tungsten by SEM, EDS, XPS and Raman. Based on above experiments, a two-stage decomposition process of SF_6 with tungsten was proposed: the first stage is the surface vulcanization reaction $W+SF_6{\rightarrow}WS_2$, mainly taken place at 600 ℃, with the activation energy valued at 152.8 kJ·mol^{-1}, according to Avrami-Erofeev equation; the second stage is the endothermic fluorination reaction $WS_2+SF_6{\rightarrow}WF_6$, mainly taken place at 750 ℃,, with the activation energy valued at 126.0 kJ·mol^{-1}, according to the Avrami-Erofeev equation.

1 Introduction

SF_6 is a synthetic inert gas, colorless, tasteless, non-toxic, with excellent insulation performance, and has been applied in many important fields including gas insulated switchgear, semiconductor processing, aerospace etc [1]. On the other hand, SF_6 is a greenhouse gas, whose threat to the environment is 23900 times that of CO_2[2]. Therefore, its extensive use has attracted many researchers to understand its chemical properties. In contrast to the widely believed chemical inertia, SF_6 can react with some compounds like metal or low-valent complex under regular conditions. For example SF_6 can react with hot sodium film at 200 ℃ [3]. At -61 ℃, SF_6 can be reduced with element Cs to CsS_2 in liquid ammonia [4]. Basta et al. found that the reaction of organotitanium and organozirconium complexes with SF_6 could react quickly at room temperature or even below room temperature [5]. Metal tungsten is a key material in electronic and electrical equipment, widely used in high voltage circuit breakers and plasma etching. Due to close contact of tungsten with SF6 under these harsh conditions, decomposition of SF6 inevitably taken place. For example, SF_6 corrodes copper-tungsten alloy and generates WF_6 under the action of arc[6]. SF_6-O_2 plasma corrodes refractory metal W to generate WF_6, WO_3, and WOF_4 [7], and Peignon et al. believed that WS_2 was an important intermediate for further oxidation or fluorination to obtain aforementioned decomposition products[8]. Fluoridation, vulcanization and oxidation occur during tungsten and SF_6 plasma etching [8-11]. At present, although researchers have basically confirmed the decomposition products of SF_6 caused by tungsten, the relevant decomposition processes are still unclear. Thermal decomposition reaction is a classical method to study the transformation of substances, which can reveal the thermodynamics and dynamics of the transformation process. However, the apparent activation energy and thermal decomposition kinetics of SF_6 reaction with tungsten powder have not been reported. Herein we adopt synchronous thermogravimetric/differential scanning calorimetric technique investigated thermal decomposition reaction of SF_6 and tungsten powder. Based on the principle of thermal analysis kinetics, the reaction temperature of W powder in SF_6 atmosphere was determined, the apparent activation energy of the reaction was calculated, and the kinetic equation of thermal decomposition reaction was obtained. Meanwhile, the decomposition product and the change of microstructure and composition at high temperature was determined by means of environmental scanning electron microscope (SEM), X-ray energy spectrum analysis (EDS), X-ray photoelectron spectrometer (XPS) and Raman spectroscopy characterization.

2 Experimental parts

2.1 The raw material

SF6 gas purity 99.99% purchased Chengdu Kemet Special Gas Co., LTD., 4-6 μm tungsten powder.

---

*
Corresponding author: Weiqiang Zhang: zwq@snnu.edu.cn, Yajun Jian: yajunjian@snnu.edu.cn; [+] These authors contributed equally to this work.

2.2 Thermal decomposition reaction of SF$_6$ and tungsten powder

The thermal decomposition behavior of SF$_6$ and tungsten was monitored by HCT-4 comprehensive thermal analyzer(Beijing Hengjiu Experimental Equipment Co., LTD.) to obtain the kinetic equation under following conditions: α-Al$_2$O$_3$ crucible was used as the reference, the gas flow rate was 100 mL·min^{-1}, sample dosage was 30-50 mg, the heating rate was 5, 10, 20 ℃·min^{-1}, and the sample pool was α-Al$_2$O$_3$, the temperature range was 25~900℃, and the temperature is ventilated at room temperature for 60 min to ensure that the furnace is filled with SF$_6$ gas and then the samples are tested by TG and heat flow at different heating rates.

2.3 Preparation of thermal decomposition reaction products

Solid decomposition products were obtained under constant temperature: under the atmosphere of SF$_6$, Al$_2$O$_3$ crucible was used as the reference, the flow rate was 100 mL · min^{-1}, and the furnace was ventilated at room temperature for 60 min to ensure that the furnace was filled with SF$_6$ gas, and the heating rate was 30 ℃·min^{-1} to 615 ℃ for 60 min, to make sure SF$_6$ and tungsten powder react completely. Solid samples were collected for further characterization after the reaction.

2.4 Characterization of solid decomposition products

The morphology and size of decomposition products were characterized by Quanta 200 environmental scanning electron microscope and EDS spectroscopy, with the parameter accelerating voltage at 20 kV and accelerating current at 2 µA. The chemical composition and element binding state of the products were analyzed by Axis UltraDLD X-ray photoelectron spectroscopy (Shimadzu, Japan), and the energy reference was stained carbon C1s (Eb=284.6 eV). The chemical composition was identified by a Reflex laser Raman spectrometer with a transmittance efficiency greater than 30%, scanning range 100-4000 cm^{-1}, signal to noise ratio of silicon third-order peak was better than 22:1 and spectral resolution as visible full spectrum ≤1 cm^{-1}.

3 Discussion of results

3.1 Thermal decomposition reaction of SF$_6$ and tungsten powder

High voltage circuit breaker contacts are mainly composed of tungsten, but the research on the chemical reaction of tungsten in SF$_6$ atmosphere is not clear, and current research mainly focuses on the plasma etching of SF$_6$ and tungsten. In order to study the reaction mechanism of SF$_6$ and tungsten at high temperature, a thermal decomposition reaction model of SF$_6$ and

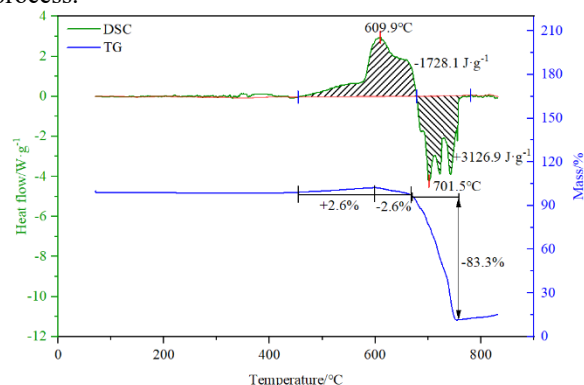tungsten powder was established to study the reaction process.

Fig.1 Thermal decomposition reaction of W powder in SF$_6$ atmosphere

It can be seen from Fig 1 that under SF$_6$ atmosphere, when heated at a heating rate of 5 ℃·min^{-1}, the weight gain of the substance occurs in the range of 457-598 ℃ with a weight gain rate of 2.6%, and the weight loss of the substance occurs in the range of 598-678 ℃ with a weight loss rate of 2.6%. The weight gain rate is basically the same as the weight loss rate. The maximum exothermic peak appears on the DSC curve at 609 ℃, which may be due to the sulfide reaction W+SF$_6$→WS$_2$ on the surface, and the heat release is 1728.1 J·g^{-1}. Substantial weight loss occurs at 678-754 ℃, with a loss rate of 83.3%. At 702 ℃, an endothermic peak appears on the DSC curve, which may be caused by surface fluoridation WS$_2$+SF$_6$→WF$_6$, the heat absorption is 3126.9 J·g^{-1}.

3.2 Characterization of solid products of thermal decomposition of SF$_6$ and tungsten powder

The morphology and elements of raw materials of tungsten powder and solid products after thermal decomposition reaction of SF$_6$ and tungsten powder were analyzed by environmental scanning electron microscopy (SEM) energy spectrum analyzer. The results are shown in Fig 2. Fig 2a shows the raw material of 4-6 µm tungsten powder, which is distributed in irregular polygons. Fig. 2b shows the scanning electron microscopy of solid decomposition products of 4-6 µm tungsten powder at 615 ℃ for 60 min. Compared with unprocessed tungsten powder, smaller particles in µm magnitude are generated on the surface, indicating that tungsten powder has undergone chemical reaction with SF$_6$. Fig. 2c shows the EDS spectra of 4-6 µm tungsten powder raw material, containing only W element. Fig. 2d shows the EDS diagram of tungsten powder at 615 ℃ for 60 min, which shows that the measured sample contains W, S and O elements, and their mass ratios are 76.91%, 17.06% and 6.03%, respectively. It is speculated that oxides and sulfides may be generated.
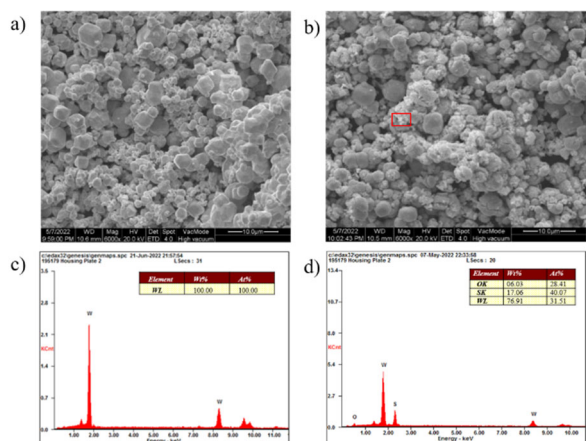
Fig.2 SEM-EDS of tungsten powder raw material, solid products after thermal decomposition reaction of SF$_6$ and tungsten powder

(**Fig. 2a** raw material of 4-6 μm tungsten powder; **Fig. 2b** SEM images of the solid decomposition products of 4-6 μm tungsten powder at 615 ℃ for 60 min. **Fig. 2c** EDS spectra of 4-6 μm tungsten powder raw materials. **Fig. 2d** EDS diagram of tungsten powder at 615 ℃ for 60 min.)

Fig. 3 shows the typical Raman spectra of the solid products of SF$_6$ reacting with W powder under 532 nm laser excitation in the frequency range of 100-800 cm^{-1}. WS$_2$ has 10 Raman modes, labeled as first-order modes of LA(M), LA(K), E$^1_{2g}$(Γ) and A$_{1g}$(Γ), second-order modes of 2LA(M) and some combined modes [12-15]. E$^1_{2g}$(Γ) and A$_{1g}$(Γ) are two optical phonon modes in the center of the Brillouin region. E$^1_{2g}$(Γ) corresponds to the in-plane optical mode, and A$_{1g}$(Γ) corresponds to the out-of-plane vibration of the sulfur atom. LA(M) is a longitudinal acoustic mode at point M, which is the collective motion of atoms in the lattice in the plane, similar to sound waves. The additional peaks correspond to the multiphonon modes combined with these first-order modes. Three peaks with good resolution can be observed in Fig. 2, which are 174.1, 350.9 and 420.1 cm^{-1} corresponding to the first modes LA(M), E$^1_{2g}$(Γ) and A$_{1g}$(Γ), respectively.

In order to determine the surface chemical composition and elemental valence of SF$_6$ reacting with tungsten powder, X-ray photoelectron spectroscopy (XPS) was performed on the solid decomposition products, and the results are shown in Fig 4. It can be seen from Fig. 4A that there are four elements: C, W, O and S after SF$_6$ reacts with tungsten powder. The C1s peak at 284.6 eV is derived from vacuum pollution. Fig 4b is the high-resolution map of W4f, where the characteristic peaks at 32.4 eV and 34.5 eV correspond to W4f 7/2 and W4f 5/2 of W4+ in WS$_2$, respectively. The characteristic peaks at 35.5 eV and 37.8 eV correspond to W4f 7/2 and W4f 5/2 of W^{6+} in WO$_3$, respectively. Fig 4c is the high-resolution diagram of S 2p, where the characteristic peaks at 35.5 eV and 37.8 eV correspond to W4f 7/2 and W4f 5/2 of W^{6+} in WO$_3$, respectively. Fig 4c is the high-resolution diagram of S2p, where the characteristic peaks
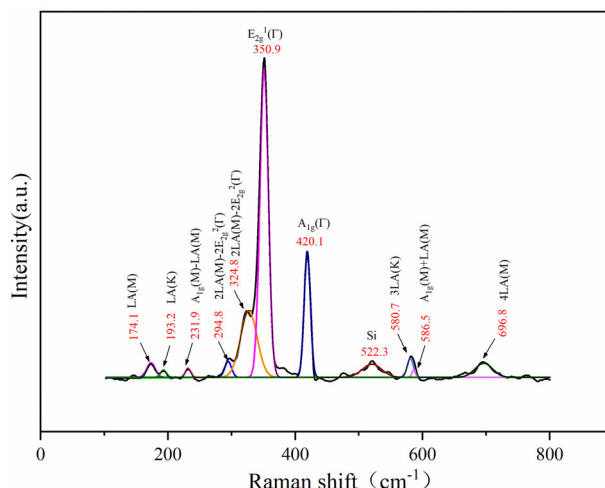

Fig. 3 Raman spectra of solid products of W powder in SF$_6$ atmosphere

at 162.0 eV and 163.3 eV correspond to S2p3/2 and S2p1/2 of S^{2-} in WS$_2$ respectively [16-18]. It is speculated that the formation of WS$_2$ is caused by the reaction between W and SF$_6$, and a small amount of WO$_3$ may be caused by the reaction between solid decomposition products and O$_2$ in the air during the cooling process, but F element is not detected, which is speculated to be caused by the volatilization of WF$_6$.
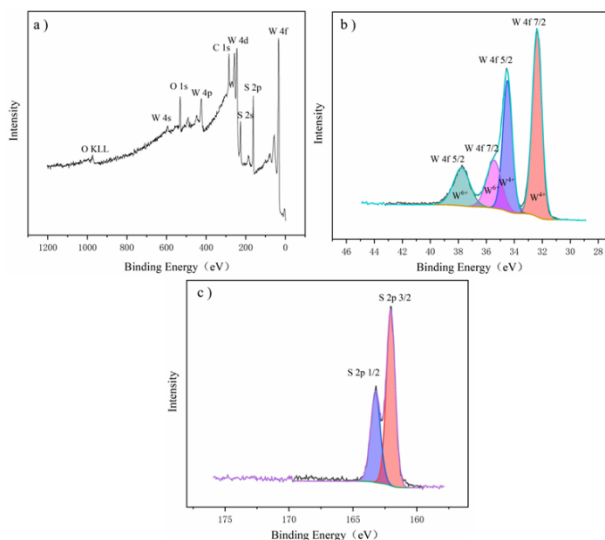

Fig. 4 XPS spectra of solid products of W powder in SF$_6$ atmosphere a) Full spectrum; b) W4f; c)S2p

3.3 Kinetic analysis of thermal decomposition reaction between SF$_6$ and tungsten powder

In order to further study the thermal decomposition reaction between SF$_6$ and tungsten powder and determine the most probable mechanism function F (α), the non-isothermal thermal decomposition kinetics of tungsten powder under SF$_6$ atmosphere was analyzed on a comprehensive thermal analyzer with different heating rates. The kinetic parameters of thermal decomposition of SF$_6$ with tungsten powder were calculated by using the Kissinger equation and the Flynn-Wall-Ozawa equation.

Table 1 shows the kinetic parameters of the thermal decomposition of SF_6 and tungsten powder calculated at different heating rates (β). It can be seen from Table 1 that the activation energy of the first stage of the sulfurization reaction of SF_6 and tungsten powder is 152.8 kJ·mol^{-1}, and the activation energy of the second stage of the fluoridation reaction is 126.0 kJ·mol^{-1}.

Ti was obtained from DSC curves of thermal decomposition reaction between SF_6 and tungsten powder at different heating rates (β), and the apparent activation energy E_α corresponding to the reaction fraction α was calculated by Ozawa equation. α and E_α were used to draw $\alpha\sim T$ and $E_\alpha \sim \alpha$ curves, and the results were shown in Fig.5.

Table 1. Apparent activation energy of tungsten powder in SF_6 atmosphere at different heating rates

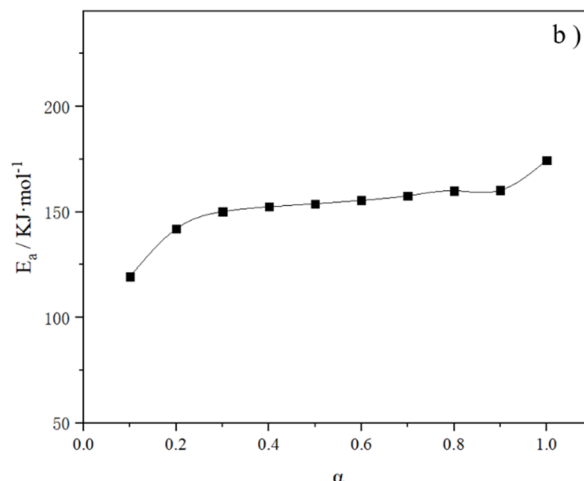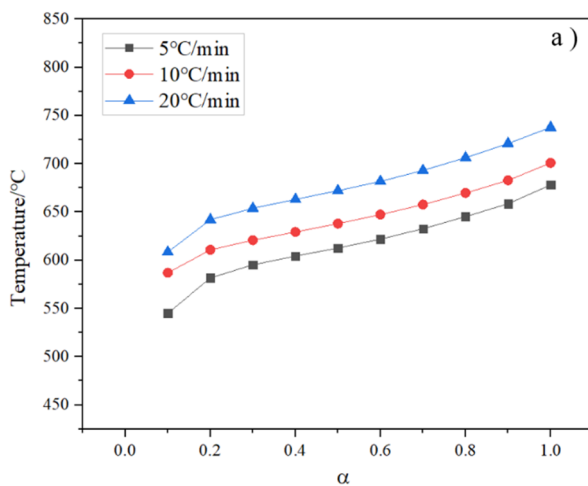| Stage	β / (°C·min^{-1})	T_p / °C	E_k / (kJ·mol^{-1})	lg(A_k / s^{-1})	r_k	E_o / (kJ·mol^{-1})	r_o
First stage	5	609	149.2	6.16	0.979	156.3	0.982
	10	627					
	20	665					
	Mean: Eo=(149.2+156.3)/2=152.8 kJ·mol^{-1}						
Second stage	5	702	120.9	3.67	0.933	131.0	0.947
	10	717					
	20	779					
	Mean: Eo=(120.9+131.0)/2=125.95 kJ·mol^{-1}						

Fig. 5a) T~α curves of SF_6 and W powder at different heating rates in the first stage of thermal reaction obtained by Ozawa method

b) E~α curve of the first stage of the thermal reaction between SF_6 and W powder obtained by Ozawa method

Table 2. calculated values of kinetic parameters for the first stage of SF_6 and W powder thermal reaction

β/ (K/min)	Eq.	E/kJ·mol^{-1}	Log (A/s^{-1})	r	Q
5	General Integral	148.13	5.93	0.999	1.63e^{-4}
	Mac-Callum-Tanner	155.37	6.46	0.999	3.03e^{-5}
	Statava-Sestak	154.87	6.44	0.999	3.03e^{-4}
	Agrawal	148.13	5.93	0.999	1.63e^{-4}
10	General Integral	152.30	6.22	0.999	2.03e^{-4}
	Mac-Callum-Tanner	159.99	6.78	0.999	3.78e^{-5}
	Statava-Sestak	159.25	6.73	0.999	3.78e^{-4}
	Agrawal	152.30	6.21	0.999	2.03e^{-4}
20	General Integral	158.08	6.51	0.999	1.61e^{-4}
	Mac-Callum-Tanner	153.501	6.78	0.999	2.89e^{-5}
	Statava-Sestak	153.112	6.78	0.999	3.00e^{-5}
	Agrawal	158.08	6.50	0.999	1.61e^{-4}
	Mean	154.42	6.44		

Stage 1: The conversion rate of 0.4-0.6 interval is different heating rate β corresponding to the thermodynamic data into the equation after the non-isothermal calculation method to obtain the activation energy Mean Eo =154.42 kJ mol^{-1}, through the Kissinger method and Ozawa method equation to calculate the activation energy Mean Eo=152.80 kJ mol^{-1}, and the activation energies are close. Table 2 shows that each G(α) and F (α) in 41 mechanism functions [19] are substituted

into the General Integral, Mac-Callum-Tanner, Statava-Sestak and Agrawal equations [20]. The kinetic parameters of thermal decomposition reaction between SF_6 and tungsten powder were determined by linear regression and logical selection. By comparison and analysis of the value of activation energy E_0, the most possible mechanism functions can be obtained as the No. 15 function. The differential formula of the mechanism function of No. 15 is $f(\alpha)=4/3[-\ln (1-\alpha)]^{1/4}$. $E_k=149.20$ kJ·mol⁻¹ and $A=10^{6.16}$ s⁻¹ calculated by Kissinger equation were substituted into equation $d\alpha/dt=(1/\beta)Af(\alpha) e^{-Ek/RT}$. The kinetic equation of the first stage thermal decomposition of SF_6 with tungsten powder is obtained as $d\alpha/dt=10^{6.16}(1/\beta) 4/3[-\ln(1-\alpha)]^{1/4} \exp(-1.492\times10^5/RT)$.
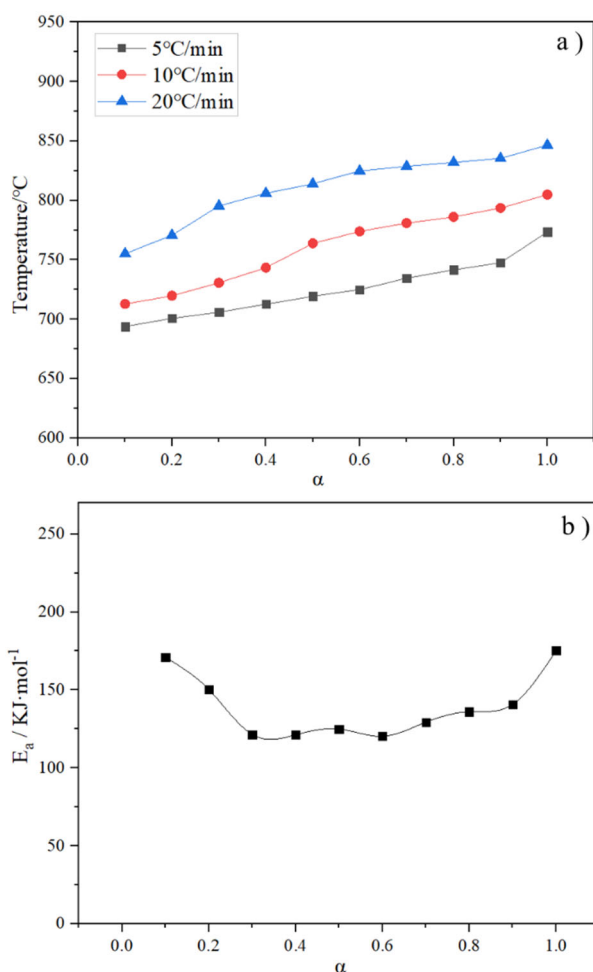

Fig. 4 a) T~α curves of SF_6 and W powder at different heating rates in the second stage of thermal reaction obtained by Ozawa method; **b)** Ozawa method obtained the E~α curve of the second phase of the thermal reaction between SF_6 and W powder

Table 4 Calculated values of kinetic parameters for the second stage of SF_6 and W powder thermal reaction

β/ (K/min)	Eq.	E/kJ·mol⁻¹	Log (A/s⁻¹)	r	Q
5	The General Integral	124.57	3.65	0.991	2.01 e⁻³
	Mac-Callum-Tanner	133.44	4.25	0.993	3.75 e⁻⁴
	Statava-Sestak	134.17	4.38	0.993	3.75 e⁻⁴
	Agrawal	124.57	3.64	0.991	2.01 e⁻³
10	The General Integral	121.82	3.28	0.990	6.90 e⁻³
	Mac-Callum-Tanner	131.25	3.90	0.992	1.30 e⁻³
	Statava-Sestak	132.10	4.05	0.992	1.30 e⁻³
	Agrawal	121.82	3.27	0.990	6.90e⁻³
20	The General Integral	118.49	3.30	0.992	1.68e⁻³
	Mac-Callum-Tanner	128.86	3.98	0.994	3.17e⁻⁴
	Statava-Sestak	129.84	4.14	0.994	3.17e⁻⁴
	Agrawal	118.49	3.29	0.992	1.68e⁻³
	Mean	126.62	3.76		

The conversion rate is 0.3-0.7 in the interval of different heating rate β corresponding to the thermodynamic data into the equation after non-isothermal calculation method to obtain the activation energy Mean Eo=126.62 kJ·mol⁻¹, through the Kissinger method and Ozawa method equation calculated the activation energy Mean Eo=125.95 kJ·mol⁻¹, and the activation energies are close. Compared with the value of activation energy E_0 calculated by 41 mechanism functions, it can be found that the most possible mechanism functions are No. 12 function. The differential formula of mechanism function No. 12 is $F(\alpha)=5/2[-\ln(1-\alpha)]^{3/5}$. $E_k=120.90$ kJ·mol⁻¹ and $A=10^{3.76}$ s⁻¹ calculated by Kissinger equation were substituted into equation $d\alpha/dt=(1/\beta)Af(\alpha) e^{-Ek/RT}$. The kinetic equation of the first stage thermal decomposition of SF_6 with tungsten powder is obtained as $d\alpha/dt=10^{3.76}(1/\beta)5/2[-\ln(1-\alpha)]^{3/5}\exp(-1.209\times10^5/RT)$.

4 Conclusion

In summary, thermal decomposition reaction of tungsten powder with SF_6 was studied through synchronous thermogravimetric/differential scanning calorimetric technique. In addition, environmental scanning electron microscope (SEM), X-ray energy spectrum analysis (EDS), X-ray photoelectron spectrometer (XPS) and Raman spectroscopy characterization was carried out for solid breakdown products under the condition of high temperature, obtaining the change of microstructure,

elements, chemical composition and structure. Based on the principle of thermal analysis kinetics, the reaction temperature of W powder in SF_6 atmosphere was determined, the apparent activation energy of the reaction was calculated, and the kinetic equation of thermal decomposition reaction was obtained. The main conclusions are as follows:

(1) Tungsten powder will interact with SF_6 at 600 ℃, and will interact with SF_6 to form WS_2 and WO_3 at 615 ℃. When the temperature reaches 750 ℃, that is, before reaching the melting and boiling point, it will evaporate completely in the form of gas WF_6.

(2) The reaction between SF_6 and tungsten can be divided into two stages. The first stage is exothermic reaction, $W+SF_6 \rightarrow WS_2$, ΔH = -1728.1 J $\cdot$ g^{-1}. The thermal decomposition kinetic equation of sulfide reaction is as follows: $d\alpha/dt=10^{6.16}(1/\beta) 4/3[-\ln (1-\alpha)]^{1/4} \exp (-1.492 \times 10^5/RT)$. The second stage is endothermic reaction, reaction equation: $WS_2+SF_6 \rightarrow WF_6$, ΔH =+3126.9 J$\cdot$g^{-1}. The kinetic equation of thermal decomposition of fluorination reaction is: $d\alpha/dt=10^{3.76}(1/\beta)5/2[-\ln(1-\alpha)]^{3/5} \exp (-1.209 \times 10^5/RT)$.

Acknowledgement

References

1. L.G. Christophorou, J.K. Olthoff, R.J. Van Brunt, IEEE Electr. Insul. Mag, 13, 20 (1997)

2. J. Zhang, J.Z. Zhou, and Q. Liu, Environ. Sci. Technol, 47, 6493(2013)

3. H. C. Cowen, F. Riding, E. Warhurst, J. Chem. Soc, 4168 (1953)

4. R. Basta, B.G. Harvey, A.M. Arif and R.D. Ernst, J. Am. Chem. Soc, 127, 11924 (2005)

5. K. Hirooka, H. Kuwahara, M. Noshiro and Y. Jitsugii, IEE Japan Trans., 95, 483 (1975)

6. W.G. Chen, L.L. Dong, et al., J. Mater., Sci. - Mater. Electron, 27, 5584, (2016)

7. A. Picard and G. Turban, Plasma Chem. Plasma Process, 5, 333 (1985).

8. M.C. Peignon, C. Cardinaud, and G. Turban, J. Appl. Phys, 70, 3314 (1991).

9. G. Turban, J.F. Coulon, Thin Solid Films, 176, 289, (1989)

10. M.C. Peignon, C. Cardinaud, G. Turban, J. Appl. Phys, 70, 3314, (1991)

11. R. Petri, D. Henry, and N. Sadeghi, J. Appl. Phys, 72, 2644, (1992)

12. N. Peimyoo, J. Shang, W. Yang, Y. Wang, C. Cong and T. Yu, Nano Res, 8, 1210, (2015)

13. A. Berkdemir, H.R. Gutierrez, A.R. Botello-Mendez, et al., Sci. Rep.-UK, 3, 1755, (2013)

14. S. Qiao, H. Yang, Z. Bai, G. Peng, X. Zhang, Proc. of the 2017 5th Int. Conf. on Mechatronics, Materials, Chemistry and Computer Engineering (ICMMCCE 2017)

15. C. Cong, J. Shang, X. Wu, et al., Adv. Opt. Mater, 2,131 (2014)

16. Tang M, Wu Y, Yang J, et al., J. Alloy. Compd, 858,157747. (2021)

17. X. Zhou, X. Yang, H. Li, et al., J. Mater. Chem, A 5, 15552 (2017)

18. Y. Yue, J. Chen, Y. Zhang, et al., ACS Appl. Mater. Interfaces, 10, 22435 (2018)

19. R.Z. Hu, Q.Z. Shi, Thermal Analysis Kinetics Beijing: Science Press (2001)

20. R.Z. Hu, Z.Q. Yang, Y.J. Liang, Thermochim. Acta, 176, 209, (1991)